Embedded fuzzy-based models in hydraulic jump prediction

Mohammad Zounemat-Kermani and Amin Mahdavi-Meymand

ABSTRACT

This study aims to evaluate the learning ability and performance of five meta-heuristic optimization algorithms in training forward and recurrent fuzzy-based machine learning models, such as adaptive neuro-fuzzy inference system (ANFIS) and RANFIS (recurrent ANFIS), to predict hydraulic jump characteristics, i.e., downstream flow depth (h_2) and jump length (L_j). To meet this end, the firefly algorithm (FA), particle swarm algorithm (PSO), whale optimization algorithm (WOA), genetic algorithm (GA), and moth-flame optimization algorithm (MFO) are embedded with the fuzzy-based models, which represent the main contribution of this study. The analysis of the results of predicting hydraulic jump characteristics shows that the embedded ANFIS and RANFIS models are more accurate than the empirical relations proposed by the previous researchers. Comparing the performance of the embedded RANFISs and ANFISs methods in predicting L_j represents the superiority of the RANFIS models to the ANFISs. The results of the sensitivity analysis show that among the input independent parameters, flow discharge (Q) is the most important factor in predicting downstream flow depth in weak, oscillating, and steady hydraulic jumps (1.7 < Froude number < 9), while the upstream flow depth (h_1) is more important than the other input parameters in strong hydraulic jumps (Froude number > 9).

Key words | fuzzy logic, hydraulic structures, hydroinformatics, machine learning, recursive models

Mohammad Zounemat-Kermani (corresponding author)
Amin Mahdavi-Meymand
Water Engineering Department,
Shahid Bahonar University of Kerman,
Kerman,
Iran
E-mail: *zounemat@uk.ac.ir*

HIGHLIGHTS

- Modeling hydraulic jump using integrative soft computing techniques.
- Appraisal of forward and recurrent fuzzy-based models in predicting hydraulic jump characteristics.
- Application of five heuristic algorithms, including FA, PSO, WOA, GA, and MFO.
- Sensitivity analyses for the weak, oscillating, steady, and strong hydraulic jumps.

NOTATION

A_i^m	= model output	d_{50}	= median diameter of the base material
A_i^o	= observational value of a phenomenon	Fr	= the Froude number
B	= flume width	g	= the gravitational acceleration
C_1	= cognitive acceleration (related to the PSO method)	h_1	= upstream supercritical flow depth
		h_2	= downstream flow depth
C_2	= social acceleration (related to the PSO method)	h_2^*	= downstream flow depth calculated from the RANFIS model
$CRMS$	= centered root-mean-square difference	h_c	= critical depth

doi: 10.2166/hydro.2020.347

$I_1, I_2, \ldots, I_k$ = independent input parameters in RANFIS
IA = index of agreement
K_s = roughness heights
L_j = hydraulic jump length
L_r = length roller in the hydraulic jump
MAE = mean absolute error
N = number of data pieces
NSE = the Nash–Sutcliffe efficiency
Q = flow discharge
r = correlation coefficient
R = hydraulic radius
R^2 = coefficient of determination
$RMSE$ = root mean square error
S_0 = slope of the bed
SD = standard deviation
u^* = shear velocity
υ = kinematic viscosity

INTRODUCTION

Description

In open channels, depends on the ratio of inertial and gravitational forces, free-surface flow is divided into three groups, including subcritical, critical, and supercritical. Subsequently, the flow in open channels (such as rivers and spillways) can be converted from subcritical to supercritical, or from supercritical to subcritical. The depth of the flow from subcritical to supercritical often changes smoothly by passing the critical depth. A sudden transition from supercritical flow to subcritical flow is associated with a high level of turbulence and energy loss and occurs in a relatively short interval; a phenomenon called the hydraulic jump.

A hydraulic jump is a complex hydraulic phenomenon in which knowing its characteristics such as the length (L_j) and secondary depth (h_2) is a necessity for appropriate planning of different types of hydraulic structures such as stilling basins (Hager 1992; Montano & Felder 2020). In the current study, soft computing techniques are applied to predict L_j and h_2 parameters. In the following subsections, the relevant studies are mentioned and, thereafter, the objectives and contribution of the research are pointed out clearly.

Literature review

Many studies have addressed modeling hydraulic jump phenomenon using different approaches such as laboratory studies, hard computing simulations (e.g., numerical simulation), and soft computing techniques (Pagliara *et al.* 2008; Gerami Moghadam *et al.* 2019; Gu *et al.* 2019). In terms of experimental and numerical perspective, hydraulic jumps have been broadly investigated and studied over the last decades. In Table 1, a summary of some pertinent experimental and numerical studies is provided.

In accordance with the topic of this paper, pertinent published studies regarding the estimation/prediction of hydraulic jump characteristics (e.g., the jump length) using soft computing methods are mentioned. Abbaspour *et al.* (2013) employed artificial neural networks (ANNs) and genetic programming (GP) for the estimation of hydraulic jump characteristics such as the free-surface location and energy dissipation. The findings of the study showed that the estimations of the ANN and GP models were in good agreement with the measured data. Additionally, the results of the ANN and GP models were compared. It was found that the ANNs gave better results than GP models.

Karbasi & Azamathulla (2016) attempted to model the properties of hydraulic jumps over rough beds with the aid of gene expression programming (GEP) models. The performances of the GEP model were compared to empirical equations, ANN, and support vector regression (SVR). A comparison of the obtained results showed that the ANN and SVR models outperformed the GEP. Azimi *et al.* (2018a) predicted the length of hydraulic jump on rough beds utilizing an integrated model of adaptive neuro-fuzzy inference system (ANFIS) and firefly algorithm (ANFIS-FA). Kumar *et al.* (2019) applied the ANN to predict the sequent depth ratio of hydraulic jump on the sloping floor with rounded and crushed aggregates. The results indicated that the ANN model has the capability to predict the sequent depth ratio with the appropriate accuracy. For the sake of the building ANIFS structure, several effective parameters, including the relative roughness of the jump, Froude number (Fr), and sequent depth were analyzed.

Table 1 | A summary of reported studies on modeling hydraulic jump characteristics using experimental and numerical studies

Approach	Author(s)/year	Parameter	Objective of the study	Conclusion remarks
Experimental	Silvester (1964)	L_j	Estimating the hydraulic jump length (L_j) of horizontal channels	A semi-empirical solution was provided for the jump length
Experimental	Hughes & Flack (1984)	L_j, h_2	Investigating properties of the hydraulic jump over rough beds	It was concluded that bed roughness diminishes both the length and the depth of a hydraulic jump
Experimental	Hager *et al.* (1990)	L_r	Defining the length roller in the classical hydraulic jump (L_r)	Relations for design were proposed based on experiments conducted in three different channels
Experimental	Mohamed Ali (1991)	L_j	Analyzing the influence of stilling basins on the length of the jump	Providing a general formula for the length of jump on a rough bed
Numerical	Ma *et al.* (2001)	L_j, h_2, L_r	Using k–ϵ turbulence model for numerical investigation of the characteristics of submerged hydraulic jumps	Providing information regarding the turbulent structure of the hydraulic jump
Experimental	Pagliara *et al.* (2008)	h_2	Investigation of the parameters that influence the sequent flow depths and modeling the length of the hydraulic jump	The experimental data were analyzed to extract a formulation of the correction coefficient based in the bed roughness
Experimental	Abbaspour *et al.* (2009)	L_j, h_2	Studying the hydraulic jump properties effected on corrugated beds	The results indicated that the length of the jump and the downstream flow depth on corrugated beds are smaller compared to the jumps on smooth bed
Experimental	Pagliara & Palermo (2015)	L_j, h_2	Studying the hydraulic jump characteristics in rough adverse-sloped channels	A semi-theoretical predictive relationship was proposed to estimate jump characteristics for a wide range of hydraulic and geometric conditions covering both rough and smooth beds
Numerical	Bayon *et al.* (2016)	L_r, h_2	Challenging the capability of two numerical models for simulating the hydraulic jump	Both numerical models gave promising results compared to the experimental observations
Experimental	Pourabdollah *et al.* (2019)	h_2	Experimental investigation of hydraulic jump characteristics on various beds, slopes, and step heights	In addition to presenting the observed values, two analytical solutions were also developed based on the momentum equation
Numerical	Gu *et al.* (2019)	L_j, h_2	Using the SPH (smoothed particle hydrodynamics) meshless method to simulate the hydraulic jump on corrugated beds	Numerical simulations were accurate in modeling different hydraulic aspects of the hydraulic jumps

Outcomes of the study revealed that the applied integrated ANFIS-FA models were superior to the standard ANFIS model for estimating the length of the hydraulic jump. In Table 2, a summary of the published reports regarding soft computing methods in simulating hydraulic jump is given.

Objectives, novelty, and contribution

Analyzing the related subjects associated with simulating hydraulic jump using soft computing methods implies that the neural network-based models (ANNs and ANFIS) acted better than other types of soft computing methods (e.g., GEP, SVR, and GP). Besides, in recent years, the adaptive neural fuzzy inference system (ANFIS) method has been successfully used in modeling hydraulic phenomena such as scour depth at piers (Muzzammil & Ayyub 2010), daily streamflow (Li *et al.* 2018), spillways aerator air demand (Mahdavi-Meymand *et al.* 2019), and scour depth around pipelines (Sharafati *et al.* 2020a). Therefore, this method was selected for the purpose of the present study. Indeed, Azimi *et al.* (2018b) stated that integrating ANFIS with meta-heuristic algorithms would increase the competence

Table 2 | A summary of reported studies on modeling hydraulic jump characteristics using soft computing techniques

Soft computing method(s)	Author(s)/year	Parameter(s)	Objective of the study	Conclusion remarks
MLPNN	Omid *et al.* (2005)	L_j, h_2	An artificial neural network (ANN) approach was applied to model sequent depth and jump length	For the rectangular section, the neural network model successfully predicted the jump length as well as the sequent depth values
MLPNN	Naseri & Othman (2012)	L_j	In this study, an ANN technique was developed to determine the length of the hydraulic jumps in a rectangular section with a horizontal apron	A comparison between the selected ANN model and the empirical Silvester equation was also made, and the results showed that the ANN method was more precise
MLPNN/GP	Abbaspour *et al.* (2013)	L_j, h_2	ANNs and genetic programming (GP) were used for the estimation of hydraulic jump characteristics	Results showed that the proposed ANN models were much more accurate than the GP models
MLPNN/GRNN	Houichi *et al.* (2013)	L_j	Two different ANNs were implemented to model the relative lengths of hydraulic jumps	The results demonstrated that both the MLPNN and GRNN were reliable predictive tools for simulating the hydraulic jump properties
GEP/SVR/MLPNN	Karbasi & Azamathulla (2016)	L_j	Application of several soft computing models to predict characteristics of hydraulic jumps over rough beds	ANN and SVR provided better results than the GEP model
ANFIS/ANFIS-FA	Azimi *et al.* (2018a)	L_r	Evaluating the potential of FA algorithm in simulating the hydraulic jump	Integrating the FA algorithm with ANFIS made the standard ANFIS produce more accurate results
GMDH/MLPNN	Azimi *et al.* (2018b)	L_r	Estimating the roller length of hydraulic jumps on rough beds using GMDH and ANN models	The suggested soft computing models' predictions were closer to the observed values than a number of other empirical models
ANFIS/Differential Evolution	Gerami Moghadam *et al.* (2019)	L_j	A hybrid method (ANFIS-DE) was proposed for modeling hydraulic jumps on sloping rough beds	Two parameters including the ratio of sequent depths and the Froude number were identified as the most important parameters in modeling the hydraulic jump length
GEP	Azimi *et al.* (2019)	L_r	Prediction of the roller length of a hydraulic jump	A simple and practical equation was proposed for predicting the length of a hydraulic jump
MLPNN	Kumar *et al.* (2019)	h_2/h_1	Prediction of sequent depth ratio	MLPNN provided better results than empirical models
ELM	Azimi *et al.* (2020)	L_j	Prediction of hydraulic jump length on slope rough beds	The flow Froude number at upstream was introduced as the most effective parameter in predicting the jump length

MLPNN: multi-layer perceptron neural network; GP: genetic programming; GEP: Gene expression programming; SVR: support vector regression; GMDH: group method of data handling; ANFIS: adaptive neuro-fuzzy inference system; ELM: Extreme Learning Machine.

of the standard ANFIS model. As a result, the main focus of this study is laid on using different types of integrated ANFIS models in predicting hydraulic jump characteristics over rough beds.

As well, several researchers have proved that the use of recurrent machine learning models would improve the performance of the counterpart standard ones (Bhattacharjee & Tollner 2016; Murali *et al.* 2020; Wei *et al.* 2020). In other words, considering a calculated output parameter as an input parameter to the soft computing model (here h_2 as the secondary depth of hydraulic jump) can yield more precise results of the

target parameter (here L_j as the length of the hydraulic jump).

Taking into account the above-mentioned issues, the contribution of the present research can be presented into three categories. Firstly, to the best knowledge of the authors, the recurrent soft computing models have not been already applied to model the hydraulic jump phenomenon. To this end, a recurrent intelligent method was employed, and results were compared with those of the standard model. In this paper, RANFIS (recurrent ANFIS) will be applied to model the hydraulic jump length (L_j) for the first time.

Second, the use of five different types of meta-heuristic optimization algorithms in learning ANFIS and RANFIS methods and comparing their performance will be accomplished. Genetic algorithm (GA), firefly algorithm (FA), and particle swarm optimization (PSO) algorithms are well-known methods with their successful applications reported by different researchers in engineering studies, especially hydraulics (Zounemat-Kermani *et al.* 2019a; Sharafati *et al.* 2020b; Zanganeh 2020). In this study, the performance of moth-flame optimization (MFO), and whale optimization algorithm (WOA), as two of the more recent intelligent algorithms, is additionally compared to those of other algorithms. So far, the capability of these five algorithms has not been assessed in engineering problems.

The third contribution of this study is associated with performing a detached sensitivity analysis in addition to the standard sensitivity analysis of the effective parameters, including discharge (Q) upstream supercritical flow depth (h_1), roughness heights (K_s), and flume width (B) by detaching the hydraulic jump into four types (weak jump, oscillating jump, steady jump, and strong jump) based on the Froude number. As an illustration, the influence of discharge is on the length of the oscillating wave is far more important than other types of jumps.

The rest of the paper is organized as follows. In the next section (Methodology section), general properties of the hydraulic jump are briefly introduced. Then, the applied empirical equations, as well as the developed soft computing methods, are described. Section 'Model implication and result' provides the mathematical and soft computing predicted results for the downstream flow depth (h_2) and hydraulic jump length (L_j) using the statistical measures and sensitivity analysis. Subsequently, in the 'Discussion' section, the Kruskal–Wallis test is used to check the significant difference between the predicted results. Finally, the 'Conclusions' section summarizes the general findings of the study applied.

METHODOLOGY

Hydraulic jump

The main characteristics of a hydraulic jump can be named as the upstream supercritical flow depth (h_1), the downstream subcritical flow depth (h_2), and the length of the hydraulic jump (the distance between the two parts (L_j)). These parameters are schematically shown in Figure 1.

In Figure 1, K_s is the roughness height of the particles in the channel bed and L_r is the roller length. As noted, in order to have a proper design of hydraulic structures like stilling basins downstream of the hydraulic jump, having the geometric characteristics of the jump is essential. In this regard, preliminary studies were carried out to provide a relationship between hydraulic jump parameters in horizontal channels with a smooth bed (Bakhmeteff 1932).

In this regard, and based on the general form of the momentum equation, the general equation for the free-surface hydraulic jump (also known as the Bélanger equation) was obtained. This equation is as follows:

$$\frac{h_2}{h_1} = \frac{1}{2}\left(-1 + \sqrt{1 + 8Fr_1^2}\right) \tag{1}$$

where Fr_1 is the supercritical Froude number of flow at the upstream and h_2/h_1 are the ratio of sequent depths.

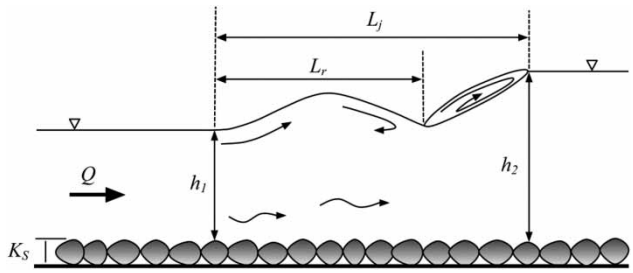

Figure 1 | Schematic section plan of hydraulic jump: L_r, Roller Length; L_j, the jump length; h_1, upstream flow depth; h_2, downstream flow depth.

The phenomenon of hydraulic jump on smooth beds has been widely studied and reported by scholars such as Peterka (1958), Rajaratnam (1967), McCorquodale (1986), and Hager (1992).

One approach to determine either the smoothness or roughness of the channel bed is taking into account the thickness of the boundary layer or Reynold's number of the particle. The thickness of the boundary layer (δ) is calculated using the following formula:

$$\delta = 11.6\frac{\upsilon}{u^*}, \quad u^* = \sqrt{RgS_0} \tag{2}$$

where υ is the kinematic viscosity, u^* is shear velocity, R is the hydraulic radius, g is the gravitational acceleration, and S_0 is the slope of the bed. If the value of bed roughness is greater than six times the thickness of the boundary layer, the bed is considered to be rough (Gadbois & Wilkerson 2014). Here, Reynold's number greater than 70 suggests the presence of a rough flow (Singh *et al.* 2007). However, studies of the hydraulic jump on rough beds have been addressed less than those on the smooth beds.

The preliminary researches on hydraulic jump on the rough beds were carried out by Rajaratnam (1968). The overall results of the researches indicated that the hydraulic jump on the rough bed creates a smaller downstream subcritical flow depth than that in which the bed is smooth (Carollo *et al.* 2007). Experimental studies indicated that the downstream depth of the jump on the rough bed is virtually half of the smooth bed (Ead & Rajaratnam 2002).

Empirical equations

Several researchers conducted studies for representing empirical relations for calculating sequent depths of hydraulic jump. Carollo *et al.* (2007) studied the hydraulic jump on several rough horizontal beds and presented a novel relation for the momentum equation for the ratio of sequent depths and the roller lengths. Pagliara *et al.* (2008) tested and analyzed the hydraulic jump properties on a rough bed and provided experimental relationships for these characteristics. In this section, the five empirical relations for predicting the downstream subcritical flow depth (h_2) and one empirical relation for estimating the length of the jump are presented in Table 3.

In the aforementioned equations, Fr_1 is the upstream Froude number, h_1 and h_2 are upstream supercritical and downstream subcritical flow depth, K_s denotes the

Table 3 | The empirical equations for estimating the h_2 (downstream flow depth) and L_j (the jump length) used in this study

Equation	Presented by	Remarks
$\frac{h_2}{h_1}=\frac{1}{2}\left(-1+\sqrt{1+8Fr_1^2}\right)$	Leutheusser & Kartha (1972)	The general quadratic equation for hydraulic jump
$\frac{h_2}{h_1}=\frac{1}{2}\left(-1+\sqrt{1+\alpha Fr_1^2}\right)$; $\alpha=7.43$, based on Carollo & Ferro (2004)	Govinda Rao & Ramaprasad (1996)	A developed form of the general jump equation
$\frac{h_2}{h_1}=\frac{1}{2}\left(-1+\sqrt{1+8\left(1-0.42\frac{K_s}{h_1}\right)Fr_1^2}\right)$	Carollo & Ferro (2004)	Jump on rough horizontal beds
$\frac{h_2}{h_1}=\frac{1}{2}\left[-1+\sqrt{1+8\left(1-\frac{2}{\pi}\arctan\left[0.8\left(\frac{K_s}{h_1}\right)^{0.75}\right]\right)Fr_1^2}\right]$	Carollo *et al.* (2007)	Jump on horizontal rough beds
$\frac{h_2}{h_1}=\frac{1}{2}\left[-1+\sqrt{1+8(3.32^{1.52S_0}Fr_1)^2\left[1+0.14\left(1-e^{2.38\frac{d_{50}}{h_c}}\right)\right]}\right]$	Pagliara & Palermo (2015)	Flows over rough beds
$\frac{L_j}{h_1}=9.75(Fr_1-1)^{1.01}$	Silvester (1964)	Hydraulic jump over horizontal channels

roughness height, d_{50} is the median diameter of the base material, h_c is the critical depth, and S_0 is the channel bed slope.

Soft computing techniques

In this study, the methods employed to predict the secondary depth are divided into two groups: soft computing based (ANFIS models) and empirical ones (see Table 3). Moreover, the methods for predicting the length of the jump are divided into two groups: soft computing based (ANFIS and RANFIS models) and one empirical relation (see Table 3). Today, many optimization algorithms have been developed to determine the relative and absolute extrema of complex functions. In the present work, five optimization algorithms were employed for training ANFIS and RANFIS, i.e., three frequently used algorithms (GA, PSO, and FA) and two novel ones (MFO and WOA). In the following, these methods are briefly explained.

ANFIS and recurrent ANFIS models

The ANFIS is an artificial intelligence learning algorithm that was first introduced by Jang (1993). ANFIS is a soft computing model generated by the learning ability of ANNs and the fuzzy inference system (FIS). By applying the fuzzy rules and sets of membership function (MFs), ANFIS is trained in accordance with the input–output data pairs of the available problem. The structure of ANFIS consists of five consequent layers, including the (1) fuzzification, (2) applying the fuzzy rules, (3) normalizing the MFs, (4) executing the consequent part of the fuzzy rules, and (5) defuzzification. Figure 2 shows the general procedure for setting up the developed ANFIS models.

Although the high capability and robustness of feed-forward ANFIS models have been proven by numerous researchers (Rajaee *et al.* 2009; Zounemat-Kermani & Scholz 2013); however, as a result of their feed-forward structure, a major deficiency of ANFIS models is that their effectiveness is limited to static problems. Thus, ANFISs are less efficient for representing dynamic processes in comparison with recurrent networks such as NARX models (Zounemat-Kermani *et al.* 2019b). Hence, it would be reasonable to upgrade the typical feed-forward ANFIS

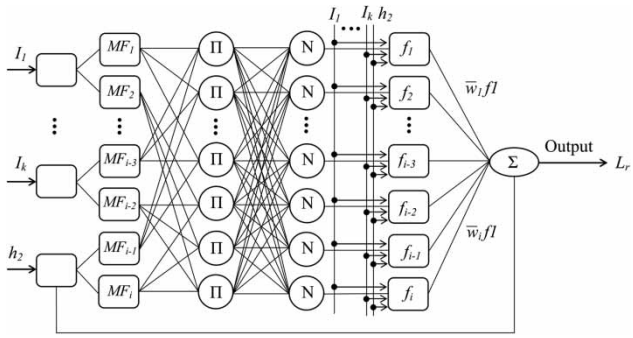

Figure 2 | Schematic plan for the architecture of the recurrent ANFIS (RANFIS) model applied.

model to a recurrent version (RANFIS) for promoting its performance in modeling recurrent problems. In this paper, as well as employing the standard feed-forward ANFIS model for predicting the downstream subcritical flow depth of jump (h_2) and the jump length (L_j), the jump length is also predicted with the predicted values for h_2 using an RANFIS model. Figure 2 shows the constructed RANFIS structure with four independent inputs and one recurrent input in this study.

In this study, $I_1, I_2, \ldots, I_k$ denote the independent input parameters such as Q, K_s, B, and h_1.

In this study, for converting the feed-forward ANFIS architecture to the recurrent ANFIS (RANFIS) type in predicting the jump length, the output of typical ANFIS $L_j = f(Q, h_1, B, K_s)$ will be changed to $L_j = f(Q, h_1, B, K_s, h_2)$ for the RANFIS. As shown in Figure 2, the output of the feed-forward ANFIS (h_2) is fedback to the input vector of the network.

Particle swarm optimization algorithm

The PSO proposed by Kennedy & Eberhart (1995) is a general random (stochastic) optimization method based on swarms such as the social behavior of birds, herds, and insects. In this method, a group of animals/insects randomly search for food in a space in which only one particle of food exists. None of the birds knows the location of the food. One of the best strategies to solve such problems is to follow birds that have the shortest distance from the food. This strategy is, in fact, the basis of the PSO algorithm. The main advantage of this method over other optimization strategies is the presence of a large number of swarming particles in it that

leads to its flexibility against the problem of local optima entrapment. Instead of using mutation, this method exchanges information among the members of the population, i.e., particles in the group. In fact, each particle regulates its path with respect to its previous best location, and the previous best location obtained by its neighbors (Hang *et al.* 2016).

Firefly algorithm

FA was introduced by Yang (2010) as a multi-factor solution to difficult optimization problems. In this algorithm, the firefly attracts other fireflies using light signals. The artificial firefly defined in this algorithm is unisex, and one firefly can attract all other fireflies. The attraction is proportional to the level of brightness of each firefly; in other words, a firefly with less brightness is less attractive, and the one with more brightness is more attractive. Fireflies with less brightness are attracted by those with higher brightness. However, if there is no firefly brighter than the present firefly, the movement of fireflies will be random. This level of brightness is defined based on the objective function: Any firefly that maximizes/minimizes the objective function based on the problem requirements has further brightness and, thus, higher attraction. On the other hand, any firefly that minimizes/maximizes the problem has less brightness and, therefore, less attraction compared to others (Zhang *et al.* 2018).

Genetic algorithm

GA was first proposed by Holland (1975). This algorithm belongs to the group of random optimization algorithms that are proper for the optimization of complex problems with unknown search space. The main idea behind GA is Darwin's theory of evolution. This theory proposes that natural attributes that are more compatible with natural rules have a higher survival chance. Since GA does not have constraining assumptions regarding the search space, it is an effective and useful method for solving optimization problems (Cheong *et al.* 2017). In GA, first, a random set of solutions is generated as the initial population that is replaced by a new candidate in each generation. In each iteration of the algorithm, the population is evaluated by the objective function, and a number of the best candidates are selected for the following generation, creating a new population. In the next step, a number of members of this population are used for generating new children by genetic operators such as crossover and mutation. These steps are iterated until the algorithm reaches the appropriate solution.

Moth-flame optimization algorithm

MFO algorithm was introduced by Mirjalili (2015) inspired by moths. Moths show an interesting method for flying at night using moonlight. Their orientation mechanism is called the transverse orientation. For flight on a straight path, moths move by maintaining a fixed angle relative to the moon. Because the moon is far from them, the path will be straight. However, it is usually observed that moths move in a spiral form around artificial lights because of the weakness in transverse orientation when the flame is near. Thus, this method is useful only when the flame is located far away. In the MFO algorithm, primary solutions are the population of moths, and the same number of flames is also considered, forming two equal-sized matrices. The fitness of each matrix is determined using the introduced objective function. In this algorithm, moths and flames are both solutions to the problem that are different in terms of the method employed for updating them in each iteration. In fact, moths move in the search space, but flames are the best locations (i.e., solutions) of moths until the performed iteration. Also, the new position of moths is calculated using a spiral.

Whale optimization algorithm

WOA is inspired by humpback whales. The behavior of these whales while hunting, which is called the bubble-net feeding method, was mathematically modeled by Mirjalili & Lewis (2016), and the WOA algorithm was extracted. Humpback whales prefer to hunt groups of plankton and small fish near the water surface. Hunting is performed by creating bubbles along the diameter of a circle or other forms. WOA considers the best solution from the primary population based on the objective function as the location of the prey or its surroundings. The other whales update their position toward this position. The location of the solution must be updated at the end of each iteration of the algorithm. WOA simulates exploitation and an exploration phase. The

exploitation phase consists of creating spiral bubbles around the prey and moving in this path toward the prey. The exploration phase comprises random searching for the prey (Mafarja & Mirjalili 2016). In this algorithm, instead of using a random method for discovering the prey, the location of the best solution is used to update new solutions.

Development of integrated ANFIS and recurrent ANFIS models

The standard version of ANFIS uses a combination of the gradient descent (GD) and least squares (LS) methods for adjusting the premise parameters (MFs parameters) and consequent parameters (linear parameters) for hybrid training the network in the forward and backward stages. The LS method in the forward stage is employed to adjust the consequent parameters (coefficients of the linear relation in Layer 4; see Figure 2), and then the back-propagation GD method in the backward stage is employed to determine the optimal premise parameter values (e.g., the slope, center, and width of the bell-shaped function of MFs in Layer 1; see Figure 2).

In this study, in addition to the application of a standard version of ANFIS/RANFIS models, the training parameters are also optimized by using five heuristic algorithms, including PSO, GA, FA, WOA, and MFO. From now on, these integrated models will be named as ANFIS-PSO/RANFIS-PSO, ANFIS-GA/RANFIS-GA, ANFIS-FA/RANFIS-FA, ANFIS-WOA/RANFIS-WOA, and ANFIS-MFO/RANFIS-MFO in this paper. The general procedure of applying integrated ANFIS/RANFIS models is shown in Figure 3.

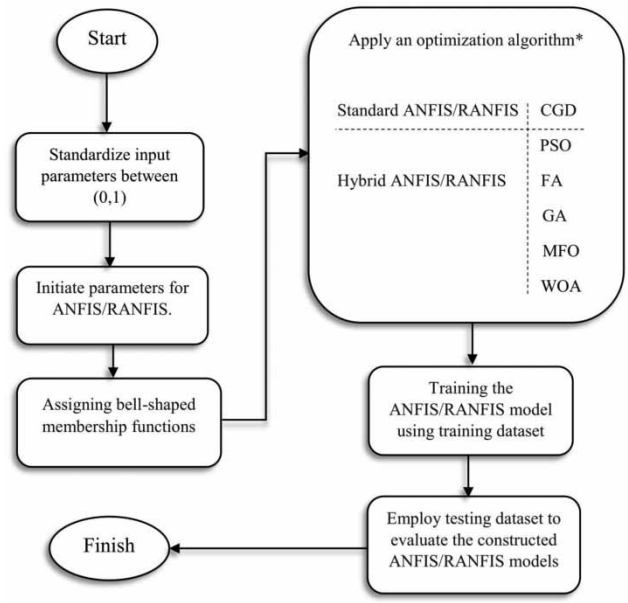

Figure 3 | General procedure for setting up the integrated ANFIS/RANFIS models.

MODEL OPTIMIZATION AND IMPLEMENTATION

Data preparation

In total, 574 data series were extracted from three reliable published scientific reports for modeling the hydraulic jump. Hughes & Flack (1984) carried out experiments on artificial rough beds and measured the characteristics of hydraulic jumps. These experiments were conducted on horizontal and rectangular flume having 0.305 m width. Five different artificially roughened beds were tested. In those experiments, the Froude number was varied from 2.34 to 10.5 and a total of 196 data under different conditions were measured. Carollo *et al.* (2007) conducted experiments on hydraulic jumps with a rough bed in a rectangular horizontal flume and measured the attributes of hydraulic jump. The flume was 14.4 m long, 0.6 m deep, and 0.6 m wide, and the Froude number was varied from 1.87 to 9.89. The number of data pieces used by these researchers was 367. Moreover, Ead & Rajaratnam (2002) performed experiments on hydraulic jump on a corrugated bed. The flume width, depth, and length were 0.446, 0.60, and 7.6 m, respectively. In their experiments, the hydraulic jump characteristics were measured under two roughened beds. The Froude number of the experiments was varied from 4 to 10, and the number of data pieces was 11. Table 4 presents a summary of the data used.

Input data

In this study, to predict the length of the hydraulic jump on a rough bed, flow rate (Q), upstream supercritical flow depth (h_1), roughness heights (K_s), and flume width (B) are calculated using the mentioned methods. In RANFIS, the downstream subcritical flow depth (h_2) enters the model as an input after the preliminary prediction. These

Table 4 | The data sources and variation ranges of data used in this study

	References		
Parameter	**Hughes & Flack (1984)**	**Ead & Rajaratnam (2002)**	**Carollo *et al.* (2007)**
Q (m^3/s)	[0.00934, 0.01472]	[0.02274, 0.09232]	[0.01736, 0.07316]
h_1 (m)	[0.0125, 0.0384]	[0.0254, 0.0508]	[0.0111, 0.0709]
h_2 (m)	[0.0780, 0.1487]	[0.104, 0.31]	[0.0898, 0.2345]
L_j (m)	[0.3962, 0.8839]	[0.41, 1.29]	[0.18, 0.9]
B (m)	0.305	0.446	0.6
K_s (mm)	[0, 11.3]	13 and 22	[0, 32]
Fr	[2.34, 10.5]	[3.995, 9.996]	[1.87, 9.89]
Number of data	196	11	367

parameters are given in Figure 1. Table 5 presents the structure of the input vector of the models.

Models setup

To create a hydraulic jump model, first, the collected data were randomized and then divided into three categories of training (70%), validation (15%), and test (15%) using the cross-validation method. Next, the network was trained using training data, and validation data were used to resolve the over-training problem. Finally, the model was evaluated by comparing the results of the model and observational data in the test category. In this study, in addition to standard models of ANFIS and RANFIS, five optimization algorithms were incorporated to train ANFIS and RANFIS methods. The general characteristics and tuning coefficients of these methods are given in Table 6.

Table 5 | The input–output structure of the soft computing models as well as empirical relations created for predicting the attributes of hydraulic jump

Model	**Input parameters**	**Target**
ANFIS	Q, h_1, B, K_s	h_2
ANFIS	Q, h_1, B, K_s	L_j
RANFIS	Q, h_1, B, K_s, h_2*	L_j
Silvester (1964)	Q, h_1, B	L_j
Leutheusser & Kartha (1972)	Q, h_1, B	h_2
Govinda Rao & Ramaprasad (1996)	Q, h_1, B, α	h_2
Carollo & Ferro (2004)	Q, h_1, B, K_s	h_2
Pagliara & Palermo (2015)	Q, h_1, B, K_s	h_2

h^*_2 = downstream flow depth calculated from the RANFIS model.

Table 6 | The applied tunning parameters for the five learning algorithms embedded with the ANFIS and RANFIS used in this study

Meta-Heuristic optimization method	**Parameter**	**Value**	**Maximum epoch**
FA	Mutation Coefficient	0.2	2,000
	Attraction Coefficient	2	
	Light Absorption Coefficient	1	
	Mutation Coefficient Damping Ratio	0.98	
	Search Space Range	[−10, 10]	
PSO	Initial inertia weight	1	2,000
	Inertia Weight Damping Ratio	0.98	
	Cognitive acceleration (C_1)	1	
	Social acceleration (C_2)	2	
	Search range	[−10, 10]	
GA	Crossover	0.6	2,000
	Mutation	0.8	
	Selection Pressure	8	
	Search Space Range	[−10, 10]	
MFO	Search Space Range	[−10, 10]	2,000
WOA	Search Space Range	[−10, 10]	2,000

MODELS' EVALUATION

Statistical measures

The statistical parameters used in this study for evaluating different models include root mean square error (*RMSE*), coefficient of determination (R^2), Nash–Sutcliffe efficiency

(*NSE*), mean absolute error (*MAE*), and index of agreement (*IA*). If the model output is denoted with A_i^m and the observational value of a phenomenon with A_i^o, each parameter is calculated as follows:

$$RMSE = \sqrt{\frac{1}{N}\sum_{i=1}^{N}(A_i^m - A_i^o)^2} \tag{3}$$

$$R^2 = \frac{\left(\sum_{i=1}^{N}(A_i^m - \overline{A^m})(A_i^o - \overline{A^o})\right)^2}{\sum_{i=1}^{N}(A_i^m - \overline{A^m})^2 \sum_{i=1}^{N}(A_i^o - \overline{A^o})^2} \tag{4}$$

$$NSE = 1 - \frac{\sum_{i=1}^{N}(A_i^m - A_i^o)^2}{\sum_{i=1}^{N}(A_i^o - \overline{A^o})^2} \tag{5}$$

$$MAE = \frac{1}{N}\sum_{i=1}^{N}|A_i^m - A_i^o| \tag{6}$$

$$IA = 1 - \frac{\sum_{i=1}^{N}(A_i^m - A_i^o)^2}{\sum_{i=1}^{N}(|A_i^m - \overline{A^o}| + |A_i^o - \overline{A^o}|)^2} \tag{7}$$

where N shows the number of data pieces, and Bar denotes the mean of variables. Statistical parameters used here can be divided into two general categories. The smaller (and closer to zero) the *RMSE* and *MAE*, the better the performance of the model; however, the closer *IA*, R^2, and *NSE* to 1, the higher the precision of the model.

Diagnostic analysis

An effective method for identifying the efficiency of the used models is the application of the Taylor diagram, which is a method for depicting the errors of different models on one diagram. In this diagram, three statistical parameters, including centered root-mean-square difference (*CRMS*), correlation coefficient (*r*), and standard deviation (*SD*) of various models, can be observed (Taylor 2001). The closer the representative point of a method is to the point of observational data, the better its performance would be in simulating the phenomenon.

MODELS IMPLICATION AND RESULT

Results for downstream flow depth (h_2) prediction

In this study, both empirical and soft computing models were applied to predict the secondary flow depth of hydraulic jump (h_2). Results of training and validation steps for predicting the h_2 using the standard ANFIS are presented in Table 7.

Statistical measures calculated in Table 7 show that the modeling methods used here were properly trained using the laboratory input data. Even for the poorest method, R^2 was

Table 7 | Statistical indices using the applied soft computing models for modeling the secondary flow depth of hydraulic jump (h_2) in the training and validation phases

		Statistical parameters				
Stage	**Method**	***RMSE* (m)**	**R^2**	***MAE* (m)**	***NSE***	***IA***
Train	ANFIS-FA	0.0038	0.988	0.0029	0.988	0.997
	ANFIS-GA	0.0042	0.984	0.0033	0.984	0.996
	ANFIS-PSO	0.005	0.978	0.0039	0.978	0.994
	ANFIS	0.0067	0.96	0.0051	0.96	0.99
	ANFIS-WOA	0.0076	0.95	0.0058	0.95	0.987
	ANFIS-MFO	0.0083	0.94	0.0061	0.94	0.984
Validation	ANFIS-FA	0.0042	0.981	0.0014	0.981	0.995
	ANFIS-GA	0.005	0.972	0.0017	0.972	0.993
	ANFIS-PSO	0.0053	0.97	0.0019	0.969	0.992
	ANFIS	0.0067	0.951	0.0024	0.951	0.987
	ANFIS-WOA	0.0076	0.936	0.0028	0.936	0.984
	ANFIS-MFO	0.0081	0.93	0.0028	0.928	0.982

higher than 0.9, *RMSE* and *MAE* were close to 0, and *NSE* and *IA* were close to 1. Results also demonstrate that FA, GA, and PSO increased the compatibility of ANFIS with laboratory results, whereas WOA and MFO lowered the efficiency of the integrated ANFIS models compared to the standard ANFIS. These results are noticeable for both training and validation data. Among these methods, ANFIS-FA estimated h_2 in the training and validation phases with more precision. During training with this method, *RMSE* was the minimum (0.0038 m), and *NSE* was the maximum (0.988). Although the performance of methods matters in training and validation, the results of the testing phase are of special importance, serving as the main criterion for depicting the performance of various methods. Table 8 presents the results of different soft computing models (i.e., the standard ANFIS and its combination with different algorithms) and three empirical relations in predicting h_2 in the test phase.

Statistical analyses on the obtained results (Table 8) reveal that conventional ANFIS and its combination with optimization algorithms predict h_2 with higher accuracy. Mean *RMSE* was 0.013 m for soft computing models, while it was 0.019 m for the best empirical relations. Based on the calculated statistical parameters, ANFIS-FA showed the highest performance in predicting the secondary depth of the jump. For this method, *RMSE* and *MAE* equaled 0.0053 and 0.0016 m, respectively (minimum values among the applied methods). Also, R^2, *NSE*, and *IA* were 0.971, 0.975, and 0.993, respectively. PSO, FA, and GA increased the precision of ANFIS modeling by 30.263, 17.105, and 21.053%, respectively, whereas MFO and WOA reduced this precision by 10.526 and 3.947%, respectively. Another method for the analysis and evaluation of results is the use of scatter plots (Figure 4).

The scatter plots in Figure 4 depict the superior performance of soft computing models compared to experimental ones. Scatter points for these methods are closer to the 45° line compared to experimental methods. Scatter points for soft computing models are not located outside the −20% and +20% lines, while this is true for the points of some experimental methods. Scatter points for soft computing models are similar to each other in terms of dispersion, showing that they have similar performance. Still, the FA outperforms the others.

Another method to evaluate and visualize the results of various methods is plotting the Taylor diagram. Figure 5 illustrates this diagram for the predicting results of the applied models.

Based on Figure 5, the points belonging to ANFIS methods are closer to the points from the observation point, suggesting that the ANFIS and its combination with optimization algorithms outperform the empirical methods. Points belonging to soft computing models are close to each other, and some are overlapping, indicating

Table 8 | Statistical indices using the applied soft computing and empirical models for predicting the secondary flow depth of hydraulic jump (h_2) in the testing phase

	Statistical parameters						
Method	***RMSE* (m)**	**R^2**	***MAE* (m)**	***NSE***	***IA***	***RMSE* improvement %**	***RMSE* improvement %**
ANFIS-FA	0.0053	0.975	0.0016	0.971	0.993	0.871	30.263
ANFIS-GA	0.006	0.967	0.0018	0.962	0.991	0.854	21.053
ANFIS-PSO	0.0063	0.962	0.002	0.959	0.99	0.846	17.105
ANFIS	0.0076	0.944	0.0026	0.94	0.985	0.815	Base
ANFIS-WOA	0.0079	0.938	0.0027	0.934	0.984	0.807	−3.947
ANFIS-MFO	0.0084	0.931	0.0028	0.926	0.982	0.795	−10.526
Carollo & Ferro (2004)	0.0242	0.626	0.007	0.388	0.865	0.41	–
Pagliara & Palermo (2015)	0.0339	0.632	0.0116	−0.203	0.785	0.173	–
Govinda Rao & Ramaprasad (1996)	0.035	0.573	0.012	−0.316	0.768	0.146	–
Leutheusser & Kartha (1972)	0.041	0.576	0.014	−0.794	0.722	Base	–

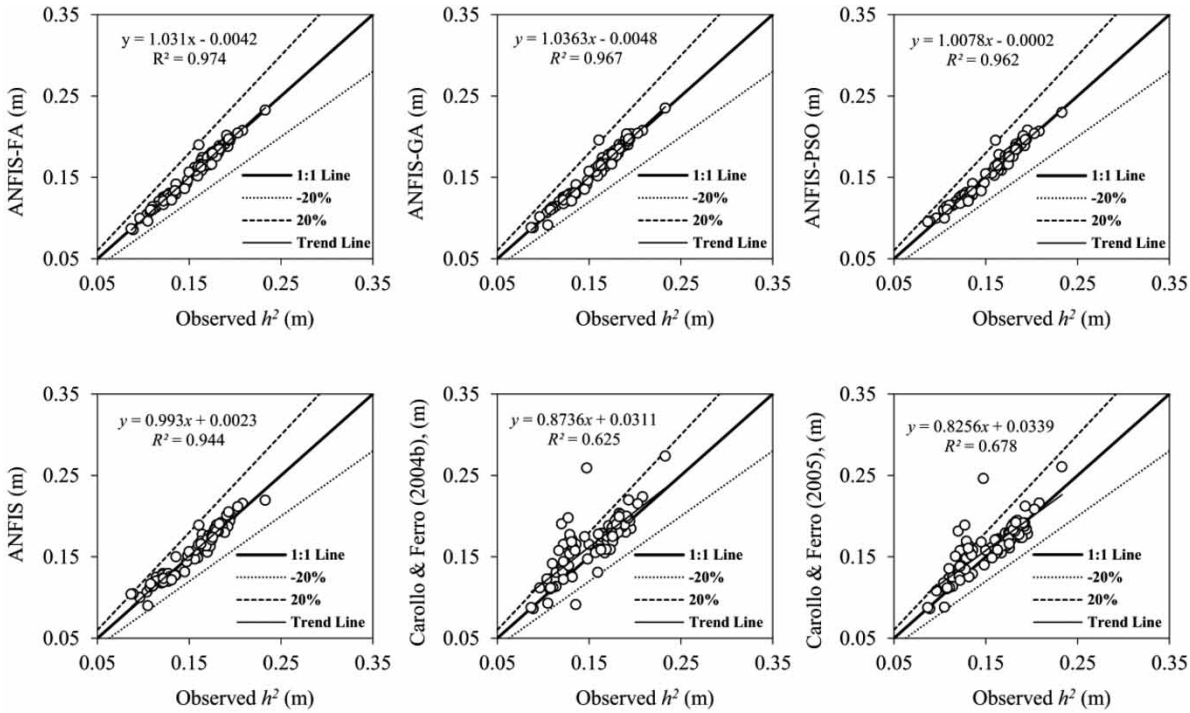

Figure 4 | Scatter plots of the predicted versus measured downstream depths of the hydraulic jumps (h_2) for the developed ANFIS models in the testing phase.

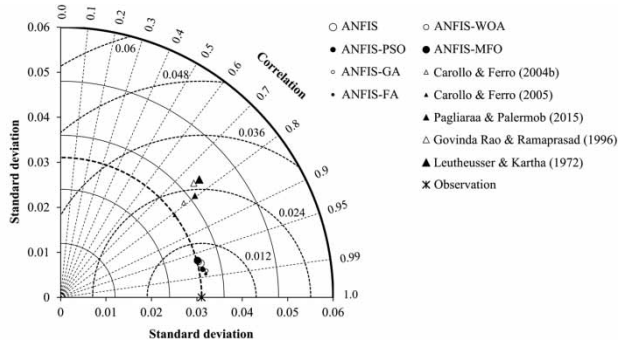

Figure 5 | Comparing performances of the empirical and soft computing (ANFIS) models in predicting h_2 using Taylor diagram.

that their output and performance are close. Still, the ANFIS-FA is closer to the observational point and outperforms the other methods.

Results for hydraulic jump length (L_j) prediction

Another parameter predicted in this research is the length of the hydraulic jump on the rough bed (L_j). This parameter is modeled using RANFIS, standard feed-forward ANFIS, and their combinations with the meta-heuristic algorithms. Table 9 presents the results of the training and validation phases for both the ANFIS and RANFIS models.

Based on Table 9, in the training and validation phases, both ANFIS and RANFIS managed to model L_j accurately. The statistical parameters show that ANFIS and RANFIS were trained similarly, such that mean *RMSE* was 0.0569 and 0.0544 m, respectively, for RANFIS and ANFIS. The performance of the optimization algorithms was similar to their performance in the previous problem (i.e., predicting the secondary depth of hydraulic jump). GA, PSO, and FA improved training, while MFO and WOA degraded it. In this step of modeling, ANFIS and RANFIS models show a similar performance. Still, ANFIS was trained better than RANFIS. The results of the testing phase based on the comparison of methods are presented in Table 10.

Based on Table 10, RANFIS has a higher precision in modeling L_j in comparison to ANFIS. Compared to ANFIS, RANFIS has a smaller *RMSE* and *MAE* (i.e., 0.0531 and 0.0178 m, respectively) and a higher *NSE*, R^2, and *IA* (0.789, 0.787, and 0.94, respectively). Among the five meta-heuristic algorithms used for training, FA, PSO,

Table 9 | Statistical indices using the applied soft computing models for modeling the hydraulic jump length (L_j) in the training and validation phases

		ANFIS			RANFIS		
		Statistical parameters			Statistical parameters		
Stage	Method	*RMSE* (m)	R^2	*IA*	*RMSE* (m)	R^2	*IA*
Train	ANFIS-PSO	0.0495	0.863	0.962	0.0497	0.861	0.962
	ANFIS-FA	0.0484	0.869	0.964	0.0506	0.857	0.961
	ANFIS-GA	0.0468	0.877	0.966	0.0501	0.859	0.961
	ANFIS	0.054	0.837	0.954	0.0562	0.823	0.949
	ANFIS-MFO	0.0577	0.813	0.946	0.064	0.771	0.931
	ANFIS-WOA	0.0705	0.721	0.914	0.0711	0.717	0.912
Validation	ANFIS-PSO	0.0432	0.887	0.97	0.0466	0.869	0.965
	ANFIS-FA	0.0498	0.849	0.959	0.0461	0.87	0.964
	ANFIS-GA	0.049	0.854	0.96	0.0531	0.829	0.95
	ANFIS	0.0527	0.831	0.953	0.0557	0.812	0.947
	ANFIS-MFO	0.0603	0.782	0.933	0.0661	0.737	0.916
	ANFIS-WOA	0.0748	0.661	0.89	0.0751	0.658	0.889

Table 10 | Statistical indices using the applied soft computing and empirical models for predicting the hydraulic jump length (L_j) in the testing phase

	Statistical parameters						
Method	*RMSE*	R^2	*MAE*	*NSE*	*IA*	*RMSE* changes %	*RMSE* improvement %
Recurrent ANFIS							
RANFIS-GA	0.046	0.846	0.016	0.841	0.960	20.86	92.03
RANFIS-PSO	0.046	0.838	0.016	0.837	0.957	20	91.94
RANFIS-FA	0.047	0.835	0.015	0.834	0.955	19.14	91.86
RANFIS	0.053	0.789	0.018	0.787	0.940	8.45	90.78
RANFIS-MFO	0.065	0.685	0.022	0.678	0.906	−12.41	88.68
RANFIS-WOA	0.074	0.599	0.026	0.588	0.880	−27.24	87.19
Conventional ANFIS							
ANFIS-GA	0.052	0.799	0.017	0.796	0.944	10.34	90.97
ANFIS-PSO	0.047	0.834	0.016	0.831	0.956	18.96	91.84
ANFIS-FA	0.048	0.827	0.016	0.824	0.953	16.72	91.61
ANFIS	0.058	0.751	0.020	0.746	0.929	*Base*	89.93
ANFIS-MFO	0.064	0.692	0.022	0.687	0.909	−10.86	88.84
ANFIS-WOA	0.074	0.598	0.026	0.587	0.879	−27.24	87.19
Empirical relation							
Silvester (1964)	0.576	0.296	0.229	−24.09	0.270	−893.10	*Base*

and GA improved the performance of both ANFIS models, whereas MFO and WOA weakened it. Figure 6 presents the scatter plot for visualizing and comparing the performance of different methods.

Based on Figure 6, the applied methods show very close performances. The scattering of points shows that recurrent methods (i.e., RANFIS) have less dispersion and, therefore, better performance compared to standard ones (i.e., ANFIS). The Taylor diagram for the length of the hydraulic jump (L_j) predicting is depicted in Figure 7.

Based on Figure 7, although the points are close to each other, RANFIS-GA was closer to the observational

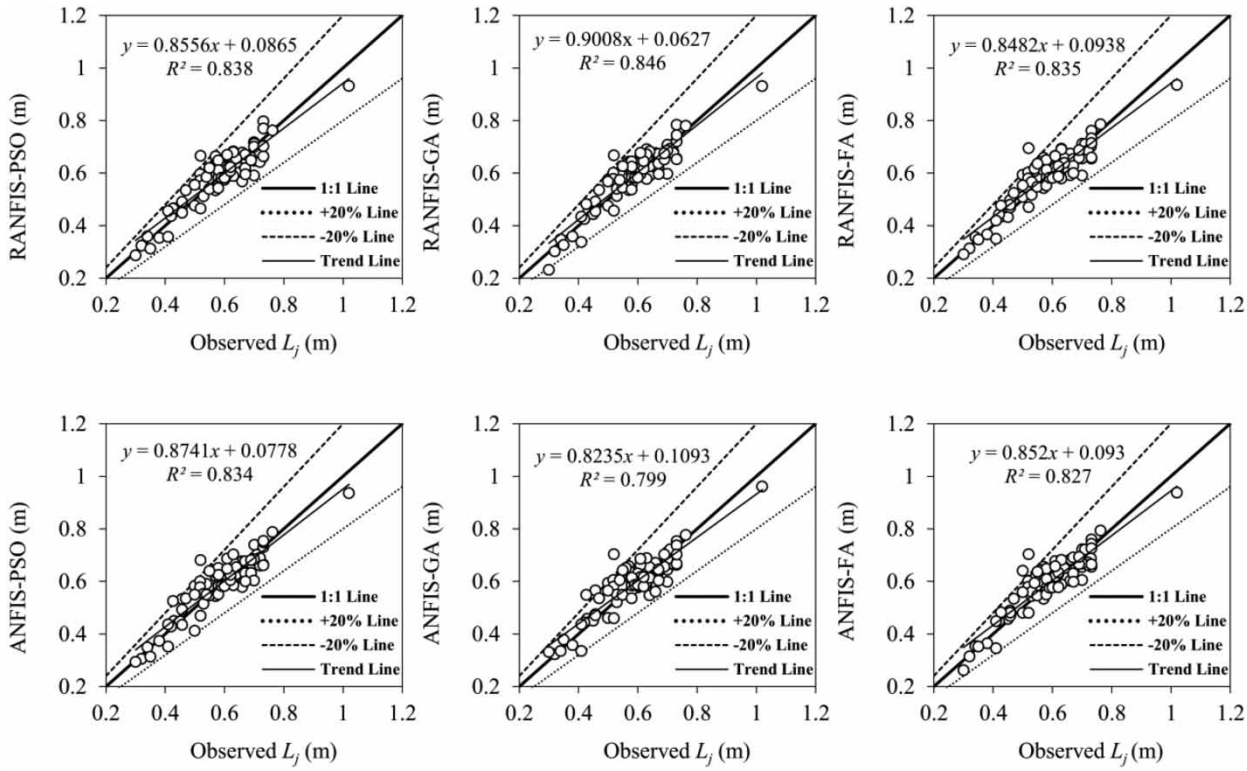

Figure 6 | Scatter plots of the predicted versus measured length of the hydraulic jumps (L_j) for the developed ANFIS and RANFIS models in the testing phase.

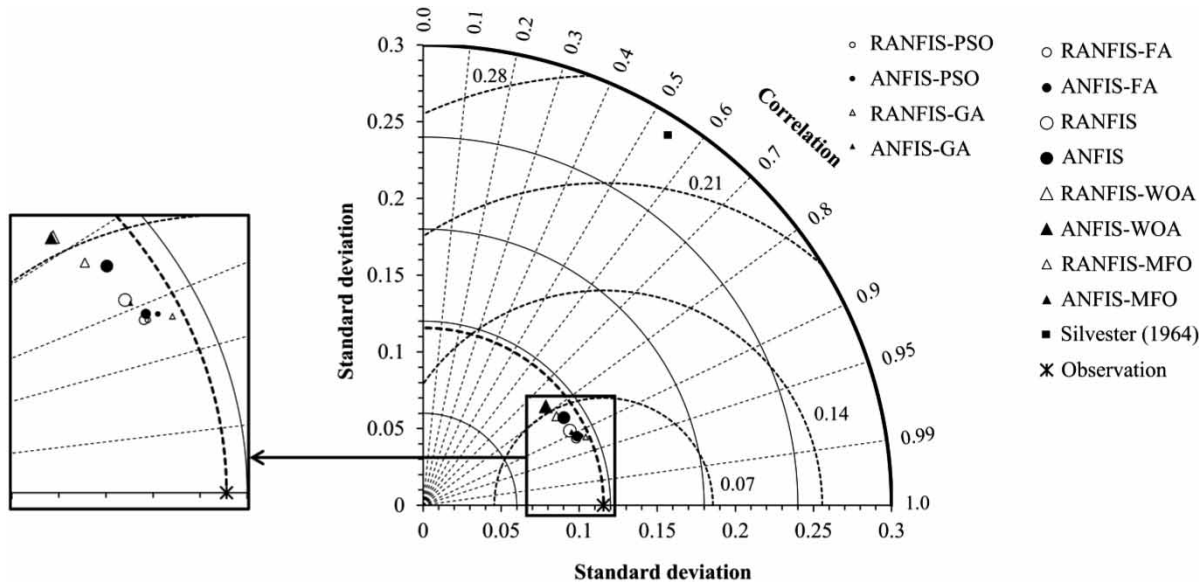

Figure 7 | Comparing performances of the empirical, ANFIS and RANFIS models in predicting L_j using Taylor diagram.

point, suggesting its superior performance compared to others. GA, PSO, and FA improved the performance of RANFIS compared to ANFIS, while the performance of MFO and WOA had a slight effect on RANFIS and even worsened it.

Sensitivity analysis

In this step, the simple correlation coefficient (*SCC*) statistical parameter was employed to examine the effect of independent input parameters on modeling and perform sensitivity analysis. Based on the Froude number, the data used for this purpose are divided into four groups (Figure 8).

This classification was performed based on the type of jump. A Froude number between 1.7 and 2.5 is a weak jump, 2.5–4.5 is an oscillating jump, 4.5–9 is a steady jump, and >9 is a strong jump.

Based on Table 4, the size of particles and width of the channel of the collected data have slight diversity; therefore, the results in Table 11 on these two parameters are not reliable. In comparison, the results for Q and h_1 are reliable. Based on Table 11, for the total data, h_1 and Q have almost equal importance in L_j modeling, but Q is more significant than h_1. For weak, oscillating, and steady jumps, the importance of Q is more than that of h_1, while the opposite is true for strong jump (with very large Froude numbers). For the case of L_j, it is found that the importance of Q is reduced by increasing the Froude number while that of h_1 is increased such that Q is more important than h_1 for weak jump, and the opposite is true for steady and strong jumps.

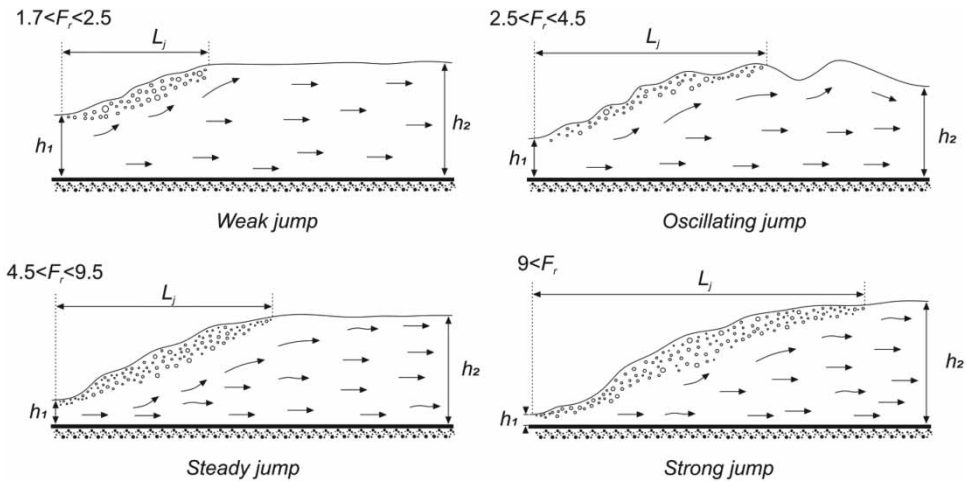

Figure 8 | Various types of hydraulic jumps based on the Froude number.

Table 11 | The results of sensitivity analysis for exploring the effectiveness of input parameters in different types of hydraulic jumps

	Hydraulic jump type									
	Nonsegregated		Weak jump		Oscillating jump		Steady jump		Strong jump	
Parameter	*SCC*-L_j	*SCC*-h_2	*SCC*-L_j	*SCC*-h_2	*SCC*-L_j	*SCC*-h_2	*SCC*-L_j	*SCC*-h_2	*SCC*-L_j	*SCC*-h_2
Q (m^3/s)	0.08	0.837	0.123	0.948	0.596	0.931	0.05	0.845	0.034	0.557
h_1 (m)	−0.102	0.456	0.058	0.866	0.543	0.764	0.264	0.724	0.816	0.81
B (m)	−0.23	0.592	−0.126	0.676	0.232	0.742	−0.327	0.557	−0.526	0.006
K_s (mm)	0.001	0.19	0.895	0.18	0.325	0.404	−0.288	0.125	−0.626	−0.122

DISCUSSION

In the previous sections, we discussed and analyzed the superior methods and parameters affecting the hydraulic jump phenomenon. Still, the question remains whether the employed methods present statistically different results for various models. To answer this question, the Kruskal–Wallis test was run over the predicted results of different applied models (Table 12).

Based on Table 12, in modeling the hydraulic jump at 95 and 99% confidence levels, no statistically significant difference exists between the results of ANFIS and RANFIS models. Furthermore, at these significance levels (0.05 and 0.01), no significant difference exists between the outputs of different algorithms. Findings on the secondary depth of jump (h_2) and jump length (L_j) show that a significant difference exists between empirical relations (see Table 3) and soft computing models results at 95 and 99% confidence levels, while no significant difference is found between the applied soft computing models.

According to the summary results in Table 2 and the outcomes of this study, soft computing models are evidently superior to experimental relations; proportional to the results of the present study. Moreover, the superiority of the FA in combination with the recurrent ANFIS compared to the standard ANFIS is in line with the results obtained in this study.

Table 12 | The results of the Kruskal–Wallis test used to determine if there were statistically significant differences between the applied predictive models

Output parameter	Applied models	*p*-value	Significantly different (95%)	Significantly different (99%)
L_j	RANFIS models	0.988	No	No
	ANFIS models	0.999	No	No
	ANFIS models, and RANFIS models	1	No	No
	ANFIS models, RANFIS models, and the empirical relation	<0.0001	Yes	Yes
h_2	ANFIS models, and the empirical relations	<0.0001	Yes	Yes
	ANFIS models	1	No	No

CONCLUSIONS

Knowing hydraulic jump characteristics is a necessity for appropriate designing and planning of hydraulic structures such as stilling basins. In this study, the most important characteristics of the hydraulic jump (L_j and h_2) on a rough bed were modeled and analyzed via ANFIS and RANFIS. In addition to ANFIS, five optimization algorithms (i.e., FA, PSO, GA, MFO, and WOA) were employed to train both ANFIS methods. To set up the ANFIS model, the input structure, including K_s, Q, h_1, and B parameters, was used. Also, to establish the RANFIS structure, the h_2 parameter as a recurrent factor was introduced to the model in addition to the mentioned inputs. The summary of the major findings of this study is presented below.

Results of h_2 modeling indicated that soft computing models are more precise than experimental ones. The calculation of error measurement parameters showed that GA, PSO, and FA enhanced the efficiency of models. Nevertheless, MFO and WOA failed to improve the performance of models. Among these algorithms, ANFIS-FA had the best performance with *RMSE*, R^2, and *IA* of 0.0053 m, 0.975, and 0.993, respectively. By considering *RMSE* as the basis, the use of GA, FA, and PSO improved the precision of ANFIS in modeling h_2 by 30.26, 21.05, and 17.10%, respectively. According to the L_j predicted outcomes, even though the prediction efficiency of ANFIS and RANFIS methods are close, the application of recurrent architecture in the RANFISs enhanced the performance of ANFISs by around 3.50% (based on the *RMSE* values). However, to have a better view and judgment about the higher performance of recurrent neuro-fuzzy models, it is suggested that RANFIS methods be used and evaluated in other engineering phenomena. The comparison of the efficiency of the heuristic algorithms demonstrated that the FA and GA have a superior performance in combination with the RANFISs. The results also indicated that the FA, PSO, and GA improve the performance of the ANFISs and RANFISs. Thus, these three algorithms are suggested to be utilized as embedded learning techniques for integrative soft computing methods in future studies.

The results of sensitivity analysis for h_2 input parameters showed that Q is more important than others in predicting

h_2 for weak, oscillatory, and steady jumps ($1.7 < Fr < 9$), while h_1 is more important for strong jumps ($Fr > 9$). In terms of L_j, by increasing the Froude number ($Fr > 9$), the importance of h_1 is increased and that of Q is decreased such that for a weak and oscillating jump, the importance of Q is higher than that of h_1, while the opposite is true for the steady and strong jump. Results of the Kruskal–Wallis test revealed that, at 95 and 99%, a statistically significant difference exists between the intelligent and experimental method in modeling h_2 ($p < 0.0001$), while no significant difference exists among soft computing models in modeling h_2 and L_j.

COMPLIANCE WITH ETHICAL STANDARDS

The authors certify that they have NO affiliations with or involvement in any organization or entity with any financial interest (such as honoraria; educational grants; participation in speakers' bureaus; membership, employment, consultancies, stock ownership, or other equity interest; and expert testimony or patent-licensing arrangements), or non-financial interest (such as personal or professional relationships, affiliations, knowledge or beliefs) in the subject matter or materials discussed in this manuscript.

DATA AVAILABILITY STATEMENT

All relevant data are available from an online repository or repositories. (https://doi.org/10.1061/(ASCE)0733-9429(1984)110:12(1755), https://doi.org/10.1061/(ASCE)0733-9429(2007)133:9(989), and https://doi.org/10.1061/(ASCE)0733-9429(2002)128:7(656)).

REFERENCES

Abbaspour, A., Dalir, A. H., Farsadizadeh, D. & Sadraddini, A. A. 2009 Effect of sinusoidal corrugated bed on hydraulic jump characteristics. *Journal of Hydro-Environment Research* **3** (2), 109–117.

Abbaspour, A., Farsadizadeh, D. & Ghorbani, M. A. 2013 Estimation of hydraulic jump on corrugated bed using artificial neural networks and genetic programming. *Water Science and Engineering* **6** (2), 189–198.

Azimi, H., Bonakdari, H., Ebtehaj, I. & Michelson, D. G. 2018a A combined adaptive neuro-fuzzy inference system–firefly algorithm model for predicting the roller length of a hydraulic jump on a rough channel bed. *Neural Computing and Applications* **29** (6), 249–258.

Azimi, H., Bonakdari, H., Ebtehaj, I., Gharabaghi, B. & Khoshbin, F. 2018b Evolutionary design of generalized group method of data handling-type neural network for estimating the hydraulic jump roller length. *Acta Mechanica* **229** (3), 1197–1214.

Azimi, H., Bonakdari, H. & Ebtehaj, I. 2019 Gene expression programming-based approach for predicting the roller length of a hydraulic jump on a rough bed. *ISH Journal of Hydraulic Engineering*, 1–11. doi:10.1080/09715010.2019.1579058.

Azimi, A. H., Shabanlou, S. & Yaghoubi, B. 2020 Prediction of hydraulic jump length on slope rough beds using extreme learning machine. *Journal of Applied Research in Water and Wastewater*. doi:10.22126/arww.2020.4427.1138.

Bakhmeteff, B. A. 1932 *Hydraulics of Open Channels*. McGraw-Hill, New York.

Bayon, A., Valero, D., García-Bartual, R. & López-Jiménez, P. A. 2016 Performance assessment of OpenFOAM and FLOW-3D in the numerical modeling of a low Reynolds number hydraulic jump. *Environmental Modeling & Software* **80**, 322–335.

Bhattacharjee, N. V. & Tollner, E. W. 2016 Improving management of windrow composting systems by modeling runoff water quality dynamics using recurrent neural network. *Ecological Modeling* **339**, 68–76.

Carollo, F. & Ferro, V. 2004 Determinazione delle altezze coniugate del risalto libero su fondo liscio e scabro. *Rivista di Ingegneria Agraria* **4**, 1–11.

Carollo, F. G., Ferro, V. & Pampalone, V. 2007 Hydraulic jump on rough beds. *Journal of Hydraulic Engineering* **133**, 989–999.

Cheong, D., Kim, Y. M., Byun, H. W., Oh, K. J. & Kim, T. Y. 2017 Using genetic algorithm to support clustering-based portfolio optimization by investor information. *Applied Soft Computing* **61**, 593–602.

Ead, S. A. & Rajaratnam, N. 2002 Hydraulic jumps on corrugated beds. *Journal of Hydraulic Engineering* **128** (7), 656–663.

Gadbois, J. & Wilkerson, G. 2014 Uniform flow development length in a rough laboratory flume. In: *World Environmental and Water Resources Congress 2014*, Portland, OR, pp. 1234–1242.

Gerami Moghadam, R., Yaghoubi, B., Izadbakhsh, M. A. & Shabanlou, S. 2019 Prediction of the hydraulic jump length on sloping rough beds using meta-heuristic neuro-fuzzy model and differential evolution algorithm. *Journal of Applied Research in Water and Wastewater* **6** (1), 8–15.

Govinda Rao, N. S. & Ramaprasad 1966 Application of momentum equation in the hydraulic jump. *La Houille Blanche* **4**, 451–453.

Gu, S., Bo, F., Luo, M., Kazemi, E., Zhang, Y. & Wei, J. 2019 SPH simulation of hydraulic jump on corrugated riverbeds. *Applied Sciences* **9** (3), 436.

Hager, W. H. 1992 *Energy Dissipaters and Hydraulic Jump*. Kluwer Academic Publisher, Dordrecht, pp. 185–224. ISBN 0-7923-1508-1.

Hager, W. H., Bremen, R. & Kawagoshi, N. 1990 Classical hydraulic jump: length of roller. *Journal of Hydraulic Research* **28** (5), 591–608.

Hang, J., Zhang, J. & Cheng, M. 2016 Application of multi-class fuzzy support vector machine classifier for fault diagnosis of wind turbine. *Fuzzy Sets and Systems* **297**, 128–140.

Holland, J. H. 1975 *Adaptation in Natural and Artificial Systems: an Introductory Analysis with Applications to Biology, Control, and Artificial Intelligence*. U Michigan Press, Ann Arbor, MI.

Houichi, L., Dechemi, N., Heddam, S. & Achour, B. 2013 An evaluation of ANN methods for estimating the lengths of hydraulic jumps in U-shaped channel. *Journal of Hydroinformatics* **15** (1), 147–154.

Hughes, W. C. & Flack, J. E. 1984 Hydraulic jump properties over a rough bed. *Journal of Hydraulic Engineering* **110** (12), 1755–1771.

Jang, J. S. 1993 ANFIS: adaptive-network-based fuzzy inference system. *IEEE Transactions on Systems, Man, and Cybernetics* **23** (3), 665–685.

Karbasi, M. & Azamathulla, H. M. 2016 GEP to predict characteristics of a hydraulic jump over a rough bed. *KSCE Journal of Civil Engineering* **20** (7), 3006–3011.

Kennedy, J. & Eberhart, R. 1995 Particle swarm optimization (PSO). In: *Proceedings of the IEEE International Conference on Neural Networks, Perth, Australia*, pp. 1942–1948.

Kumar, M., Kumar, S. & Bidhu, S. 2019 Determination of sequent depth of hydraulic jump over sloping floor with rounded and crushed aggregates using experimental and ANN model. *Water Supply* **19** (8), 2240–2247.

Leutheusser, H. J. & Kartha, V. C. 1972 Effects of inflow conditions on hydraulic jump. *Journal of the Hydraulics Division* **98** (8), 1367–1385.

Li, X., Sha, J., Li, Y. M. & Wang, Z. L. 2018 Comparison of hybrid models for daily streamflow prediction in a forested basin. *Journal of Hydroinformatics* **20** (1), 191–205.

Ma, F., Hou, Y. & Prinos, P. 2001 Numerical calculation of submerged hydraulic jumps. *Journal of Hydraulic Research* **39** (5), 493–503.

Mafarja, M. & Mirjalili, S. 2016 Whale optimization approaches for wrapper feature selection. *Applied Soft Computing* **62**, 441–453.

Mahdavi-Meymand, A., Scholz, M. & Zounemat-Kermani, M. 2019 Challenging soft computing optimization approaches in modeling complex hydraulic phenomenon of aeration process. *ISH Journal of Hydraulic Engineering*. https://doi.org/10.1080/09715010.2019.1574619

McCorquodale, J. A. 1986 Hydraulic jumps and internal flows. In: *Encyclopaedia of Fluid Mechanic*, Vol. 2, N.P. Cheremisionoff Ed., Gulf Publishing, Houston, pp. 120–173.

Mirjalili, S. 2015 Moth-flame optimization algorithm: a novel nature-inspired heuristic paradigm. *Knowledge-Based Systems* **89**, 228–249.

Mirjalili, M. & Lewis, A. 2016 The whale optimization algorithm. *Advances in Engineering Software* **95**, 51–67.

Mohamed Ali, H. S. 1991 Effect of roughened-bed stilling basin on length of rectangular hydraulic jump. *Journal of Hydraulic Engineering* **117** (1), 83–93.

Montano, L. & Felder, S. 2020 LIDAR observations of free-surface time and length scales in hydraulic jumps. *Journal of Hydraulic Engineering* **146** (4), 04020007.

Murali, P., Revathy, R., Balamurali, S. & Tayade, A. S. 2020 Integration of RNN with GARCH refined by whale optimization algorithm for yield forecasting: a hybrid machine learning approach. *Journal of Ambient Intelligence and Humanized Computing*. https://doi.org/10.1007/s12652-020-01922-2.

Muzzammil, M. & Ayyub, M. 2010 ANFIS-based approach for scour depth prediction at piers in non-uniform sediments. *Journal of Hydroinformatics* **12** (3), 303–317.

Naseri, M. & Othman, F. 2012 Determination of the length of hydraulic jumps using artificial neural networks. *Advances in Engineering Software* **48**, 27–31.

Omid, M. H., Omid, M. & Esmaeeli Varaki, M. 2005 Modeling hydraulic jumps with artificial neural networks. *Proceedings of the Institution of Civil Engineers – Water Management* **128** (2), 65–70.

Pagliara, S. & Palermo, M. 2015 Hydraulic jumps on rough and smooth beds: aggregate approach for horizontal and adverse-sloped beds. *Journal of Hydraulic Research* **53** (2), 243–252.

Pagliara, S., Lotti, I. & Palermo, M. 2008 Hydraulic jump on rough bed of stream rehabilitation structures. *Journal of Hydro-Environment Research* **2** (1), 29–38.

Peterka, A. J. 1958 *Hydraulic Design of Stilling Basins and Energy Dissipaters*. Engineering Monograph No. 25, U.S. Bureau of Reclamation, Denver, Colorado.

Pourabdollah, N., Heidarpour, M. & Koupai, J. A. 2019 An experimental and analytical study of a hydraulic jump over a rough Bed with an adverse slope and a positive step. *Iranian Journal of Science and Technology, Transactions of Civil Engineering* **43** (3), 551–561.

Rajaee, T., Mirbagheri, S. A., Zounemat-Kermani, M. & Nourani, V. 2009 Daily suspended sediment concentration simulation using ANN and neuro-fuzzy models. *Science of the Total Environment* **407** (17), 4916–4927.

Rajaratnam, N. 1967 Hydraulic jumps. *Advances in Hydroscience* **4**, 197–280.

Rajaratnam, N. 1968 Hydraulic jumps on rough beds. *Transactions of the Engineering Institute of Canada* **11** (A-2), 1–8.

Sharafati, A., Tafarojnoruz, A., Motta, D. & Mundher Yaseen, Y. 2020a Application of nature-inspired optimization algorithms to ANFIS model to predict wave-induced scour depth around pipelines. *Journal of Hydroinformatics* **22** (6), 1425–1451.

Sharafati, A., Tafarojnoruz, A., Shourian, M. & Yaseen, Z. M. 2020b Simulation of the depth scouring downstream sluice gate: the validation of newly developed data-intelligent models. *Journal of Hydro-Environment Research* **29**, 20–30.

Silvester, R. 1964 Hydraulic jump in all shapes of horizontal channels. *Journal of the Hydraulics Division* **90** (1), 23–56.

Singh, K. M., Sandham, N. D. & Williams, J. J. R. 2007 Numerical simulation of flow over a rough bed. *Journal of Hydraulic Engineering* **133** (4), 386–398.

Taylor, K. E. 2001 Summarizing multiple aspects of model performance in a single diagram. *Journal of Geophysical Research* **106**, 7183–7192.

Wei, X., Zhang, L., Yang, H. Q., Zhang, L. & Yao, Y. P. 2020 Machine learning for pore-water pressure time-series prediction: application of recurrent neural networks. *Geoscience Frontiers* **12** (1), 453–467.

Yang, X. S. 2010 *Nature-Inspired Metaheuristic Algorithms*. Luniver Press, Cambridge, UK.

Zanganeh, M. 2020 Improvement of the ANFIS-based wave predictor models by the particle swarm optimization. *Journal of Ocean Engineering and Science* **5** (1), 84–99.

Zhang, L., Srisukkham, W., Neoh, S. H., Lim, C. P. & Pandit, D. 2018 Classifier ensemble reduction using a modified firefly algorithm: an empirical evaluation. *Expert Systems with Applications* **93**, 395–422.

Zounemat-Kermani, M. & Scholz, M. 2013 Modeling of dissolved oxygen applying stepwise regression and a template-based fuzzy logic system. *Journal of Environmental Engineering* **140** (1), 69–76.

Zounemat-Kermani, M., Kisi, O., Piri, J. & Mahdavi-Meymand, A. 2019a Assessment of artificial intelligence-based models and metaheuristic algorithms in modeling evaporation. *Journal of Hydrologic Engineering* **24** (10), 04019033.

Zounemat-Kermani, M., Stephan, D. & Hinkelmann, R. 2019b Multivariate NARX neural network in prediction gaseous emissions within the influent chamber of wastewater treatment plants. *Atmospheric Pollution Research* **10** (6), 1812–1822.

First received 1 October 2020; accepted in revised form 23 November 2020. Available online 14 December 2020